LA-UR-15-22281

Title: Retuning the DARHT Axis-II Linear Induction Accelerator

Author(s): Ekdahl, Carl August Jr.
Schulze, Martin E.
Carlson, Carl A.
Frayer, Daniel K.

Intended for: Report

Issued: 2015-03-31

Retuning the DARHT Axis-II Linear Induction Accelerator

Carl Ekdahl and Martin Schulze
Los Alamos National Laboratory
Carl Carlson and Daniel Frayer
National Security Technologies, LLC

I. INTRODUCTION

The Dual-Axis Radiographic Hydrodynamic Test (DARHT) facility uses bremsstrahlung radiation source spots produced by the focused electron beams from two linear induction accelerators (LIAs) to radiograph large hydrodynamic experiments driven by high explosives. The Axis-II 1.7-kA, 1600-ns beam pulse is transported through the LIA by the magnetic field from 91 solenoids as it is accelerated to ~16.5 MeV. The magnetic field produced by the solenoids and 80 steering dipole pairs for a given set of magnet currents is known as the "tune" of the accelerator [1]. From June, 2013 through September, 2014 a single tune was used. This tune was based on measurements of LIA element positions made over several years [2], and models of solenoidal fields derived from actual field measurements [3] [4].

The Axis-2 LIA was retuned in October, 2014 to incorporate recent re-measurements of the positions of LIA cells [5], and new models of some of the solenoids based on computer simulations [5]. The new tune was designed with the XTR beam envelope code using same the initial conditions as the old tune. Using the new solenoid models and positions, the XTR result shown in Figure 1 was achieved by changing the last two solenoids in the BCUZ, all six solenoids in cell block three, and the first in cell block 4. The average change of these solenoid current settings was ~10.7%. Appendix A lists the actual magnet currents for the old and new tunes for comparison.

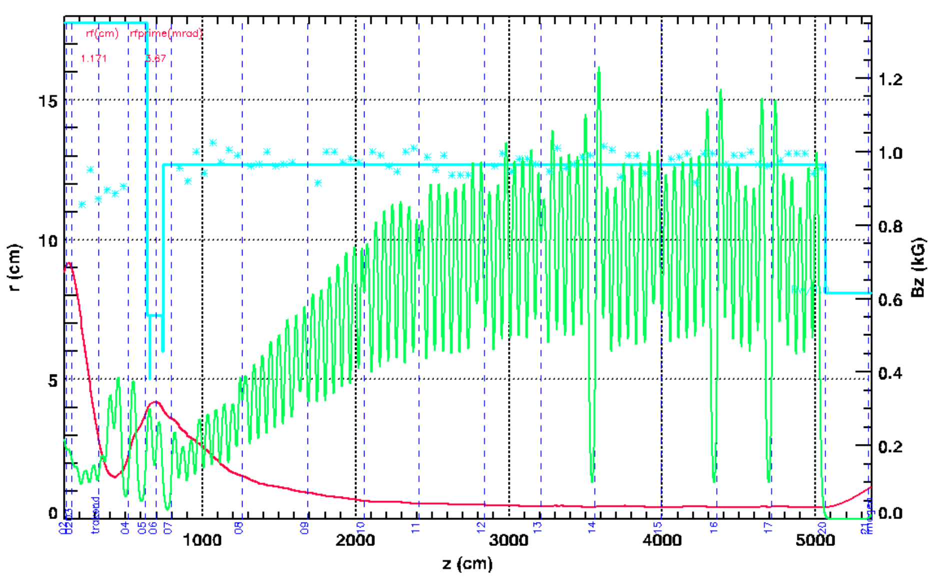

Figure 1: New tune designed with XTR for DARHT Axis-I. (Red) Beam envelope. (Green) Magnetic guide field on axis, right scale. (Solid cyan) Beam pipe wall. (Cyan asterisks) Accelerating cell potentials. (Blue dashed) BPM locations.

In addition, when the new tune was implemented on the accelerator, the second anode solenoid current was increased by ~10% (see Appendix A). Also, solenoid 65 and 72 currents were reduced by ~8.5% and ~10% respectively. Moreover, the steering dipole magnet currents were empirically adjusted to reduce beam motion at the exit [1], and the downstream transport was retuned. Therefore, differences in radiographic performance between the old and new tunes can be attributed to the following factors:

- Different solenoidal magnetic field in the accelerator
- Different magnetic field in the injector anode
- Different dipole magnetic fields in the accelerator
- Different tunes of the downstream transport elements

The first two of these might have a profound effect on envelope oscillations, and hence on emittance growth, whereas dipole fields have little effect in PIC code simulations [6]. Emittance growth in the downstream transport is unknown. We attempted to see if retuning affected the emittance by measuring it using the solenoid scan technique. We report preliminary results of those measurements in this article.

II. EMITTANCE MEASUREMENTS

We estimated the beam emittance with the focal scan technique, in which a single focusing solenoid is used to vary the beam size at a downstream imaging target. An appropriate beam optics code can then be used to find the beam initial conditions at an upstream point. In our experiments we used a solenoid 3.8 m upstream of the final focus to change the beam size at a target 1.1-m downstream. We imaged the 50-ns beam pulse produced by the kicker with the optical transition radiation (OTR) from a 51-micron-thick Ti target using a 10-ns gated camera. We then used the XTR beam-envelope code to find the beam envelope size, envelope divergence, and emittance at a position upstream of the focusing solenoid by a maximum-likelihood fit to our data. This code has been the standard for this type of analysis of data from both axes of DARHT since their inception. Since the sensitivity of the analysis to emittance is maximized by maximizing the upstream drift distance, we designated the initial position at the last focusing element; a quadrupole 3.6-m upstream of the focusing solenoid.

Maximum-likelihood fitting of data from a focal scan is dominated by the smallest beam images. Using only the data from focusing solenoid currents between 90A and 120A, the calculated emittance was within 2% of the value obtained using all of the data. The data and fits for the smallest spots are shown for the old and new tunes in Figure 2 and Figure 3 to better see several features. For example, even though the focal length giving the smallest image shifted, its size was almost unchanged. Also, the asymmetry errors in the images obtained with the new tune were substantially greater than in data obtained with the old tune. The emittance calculated from the best fits to these data was less than 4% different for the two tunes, which is less than the errors in the measurements. It follows that changing the solenoid strengths had no effect on the emittance to within the accuracy of these measurements.

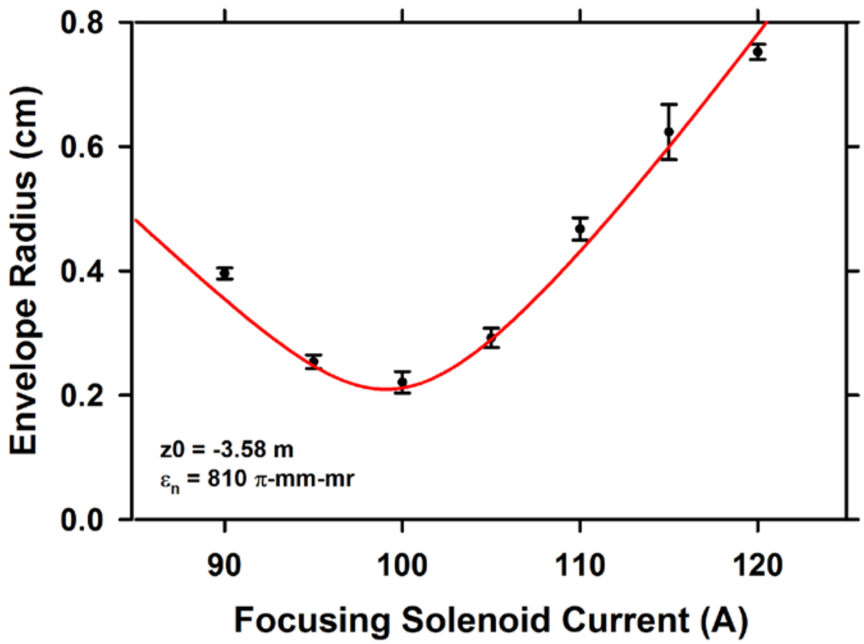

Figure 2: Data from a focal scan of the Axis-2 beam showing the fit by XTR (red line). (Focal length of the solenoid is approximately inversely proportional to its current.) These data were obtained March 3, 2014 with the old accelerator tune implemented. Error bars indicate uncertainty due to asymmetry of the images.

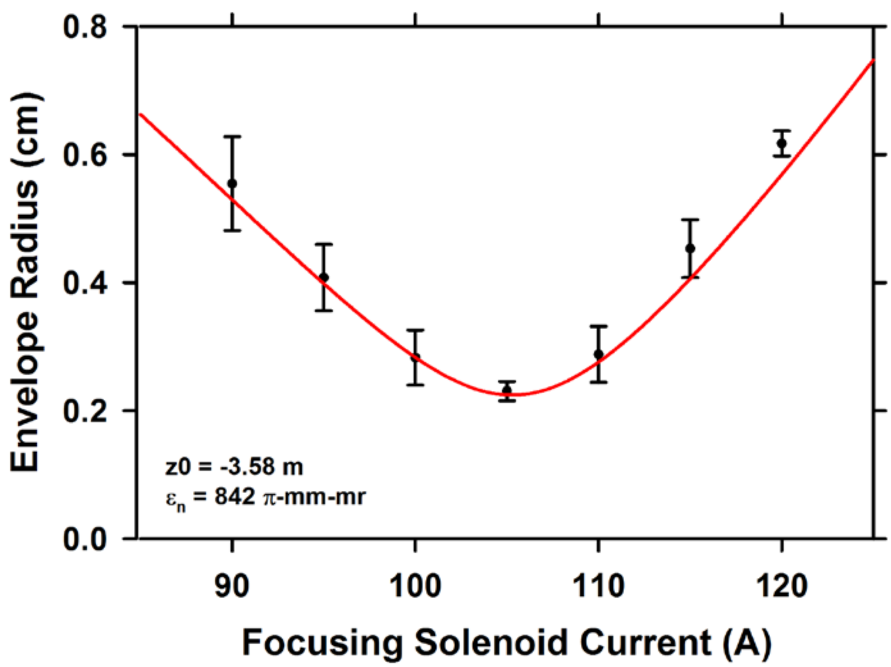

Figure 3: Data from a focal scan of the Axis-2 beam showing the fit by XTR (red line). (Focal length of the solenoid is approximately inversely proportional to its current.) These data were obtained December 9, 2014 with the new accelerator tune implemented. Error bars indicate uncertainty due to asymmetry of the images.

One drawback of this technique as originally implemented is that imaging over the full size of the target compromises measurements of the smallest sizes. This is due to the ~100:1 dynamic range of sizes and the limited number of image pixels (1000 x 1000). This limited the resolution of the smallest spots (Fig. 2 and Fig.3), adding significant uncertainty (~13% /2px) to the data. To alleviate this problem we executed a limited scan with the camera zoomed in to approximately double the magnification. The results with the new tune are shown in Fig. 4. The beam size measured with the higher magnification was significantly smaller, and fitting these data yielded a much lower emittance; 547 mm-mr. Time allotted prevented repeating this measurement with the old tune for a direct comparison.

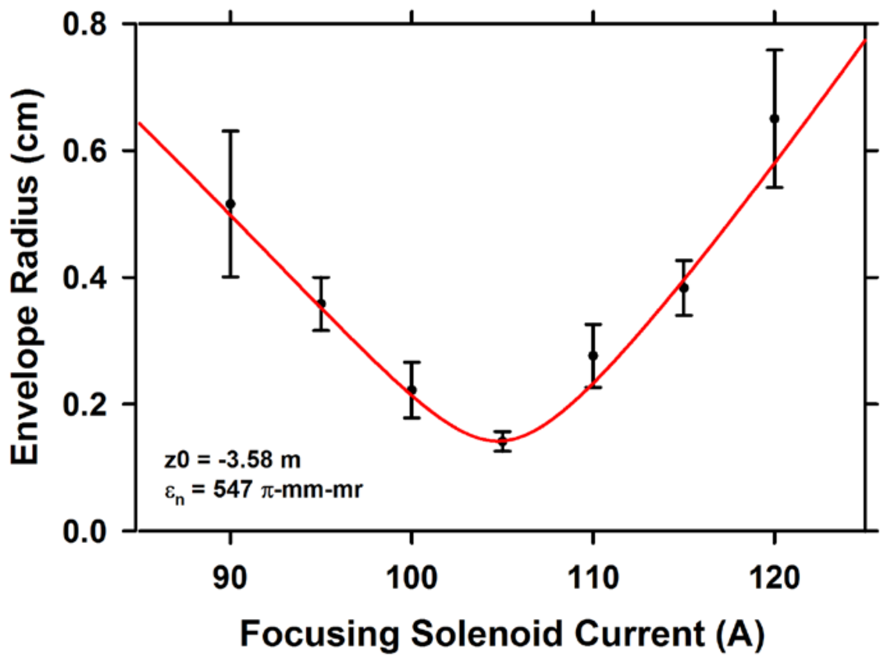

Figure 4: Data from a focal scan with higher magnification of the images. XTR fit in red. (Focal length of the solenoid is approximately inversely proportional to its current.) These data were obtained December 9, 2014 with the new accelerator tune implemented. Error bars indicate uncertainty due to asymmetry of the images.

III. CONCLUSIONS

Based on the focus scan technique, changing the tune of the accelerator and downstream transport had no effect on the beam emittance, to within the uncertainties of the measurement. Beam sizes appear to have been overestimated in all prior measurements because of the low magnification of the imaging system. This has resulted in overestimates of emittance by ~50%. The high magnification imaging should be repeated with the old tune for direct comparison with the new tune. High magnification imaging with the new accelerator tune should be repeated after retuning the downstream to produce a much more symmetric beam to reduce the uncertainty of this measurement. Thus, these results should be considered preliminary until we can effect a new tune to produce symmetric spots at our imaging station, for high magnification images.

Acknowledgements

The authors gratefully acknowledge the skilled DARHT crew for operating the Axis-II accelerator for retuning and emittance measurements.

This research was supported by the National Nuclear Security Administration of the U. S. Department of Energy under contract DE-AC52-06NA25396.

References

[1] C. Ekdahl, "Tuning the DARHT long-pulse linear induction accelerator," *IEEE Trans. Plasma Sci.*, vol. 41, pp. 2774 - 2780, 2013.

[2] H. V. Smith and et al., "As-built configuration of the 18-MeV DARHT accelerator components," Los Alamos Naional Laboratory Report LA-UR-08-08022, 2008.

[3] T. Houck, "Magnetic fields for beam transport in the DARHT-II injector commissioning," Lawrence Berkeley National Laboratory Engineering Note M8109, 2002.

[4] T. Houck, "Magnets," Personal Communication, 8/14/2002.

[5] M. Schulze, "New XTR deck and magnet models," personal communication, 3/17/2014.

[6] C. Ekdahl and et al., "Emittance growth in linear induction accelerators," in *20th Int. Conf. High Power Part. Beams*, Washington, DC, 2014.

APPENDIX A. Comparison of tunes

Hydro		4009	4011			
Tune		**OLD**	**NEW**	**Difference**	**Difference**	**|Difference|**
		A	**A**	**A**	**%**	**%**
Bucking		13.69	13.64	0.05	0.36523	
Anode	1	7.686	7.686	0	0	
Anode	2	14.46	16	-1.54	-10.6501	10.65007
Anode	3	18.78	18.78	0	0	
Begin	CB01					
Cell	1	1.884	1.884	0	0	
Cell	2	2.268	2.268	0	0	
Cell	3	2.242	2.242	0	0	
Cell	4	2.632	2.629	0.003	0.113982	
Cell	5	5.349	5.349	0	0	
Cell	6	6.914	6.914	0	0	
BCUZ	1	6.921	6.914	0.007	0.101141	
BCUZ	2	5.631	5.349	0.282	5.007991	5.007991
BCUZ	3	4.902	4.654	0.248	5.05916	5.05916
Begin	CB02					
Cell	7	3.411	3.411	0	0	
Cell	8	2.804	2.804	0	0	
Cell	9	3.064	3.064	0	0	
Cell	10	3.89	3.89	0	0	
Cell	11	4.114	4.119	-0.005	-0.12154	
Cell	12	4.273	4.273	0	0	
Cell	13	4.484	4.488	-0.004	-0.08921	
Cell	14	4.396	4.396	0	0	
InterCB		3.648	3.648	0	0	
Begin	CB03					
Cell	15	4.655	5.398	-0.743	-15.9613	15.96133
Cell	16	5.42	6.097	-0.677	-12.4908	12.49077
Cell	17	5.815	6.36	-0.545	-9.37231	9.372313
Cell	18	6.145	6.919	-0.774	-12.5956	12.59561
Cell	19	6.396	7.2	-0.804	-12.5704	12.57036
Cell	20	6.637	7.613	-0.976	-14.7054	14.70544
InterCB		8.603	8.597	0.006	0.069743	
InterCB		8.933	8.914	0.019	0.212695	
Begin	CB04					
Cell	21	9.604	10.4	-0.796	-8.28821	8.288213
Cell	22	8.945	8.941	0.004	0.044718	
Cell	23	9.407	9.402	0.005	0.053152	

Cell	24	10.84	10.84	0	0	
Cell	25	10.41	10.41	0	0	
Cell	26	11.61	11.61	0	0	
InterCB		7.947	7.947	0	0	
Begin	CB05					
Cell	27	10.43	10.43	0	0	
Cell	28	11.6	11.6	0	0	
Cell	29	12.01	12.01	0	0	
Cell	30	12.25	12.25	0	0	
Cell	31	12.4	12.4	0	0	
Cell	32	12.11	12.11	0	0	
InterCB		8.862	8.862	0	0	
Begin	CB06					
Cell	33	11.23	11.21	0.02	0.178094	
Cell	34	13.09	13.09	0	0	
Cell	35	13.07	13.06	0.01	0.076511	
Cell	36	12.69	12.69	0	0	
Cell	37	12.91	12.93	-0.02	-0.15492	
Cell	38	12.75	12.76	-0.01	-0.07843	
InterCB		15.97	15.97	0	0	
InterCB		16.15	16.11	0.04	0.247678	
Begin	CB07					
Cell	39	12.48	12.48	0	0	
Cell	40	13.16	13.18	-0.02	-0.15198	
Cell	41	14.76	14.76	0	0	
Cell	42	13.97	13.97	0	0	
Cell	43	16.99	16.99	0	0	
Cell	44	14.44	14.44	0	0	
InterCB		10.23	10.23	0	0	
Begin	CB08					
Cell	45	11.96	11.96	0	0	
Cell	46	15.27	15.27	0	0	
Cell	47	14.08	14.09	-0.01	-0.07102	
Cell	48	14.25	14.25	0	0	
Cell	49	14.15	14.15	0	0	
Cell	50	15.91	15.92	-0.01	-0.06285	
Begin	CB09					
Cell	51	17.97	17.96	0.01	0.055648	
Cell	52	12.88	12.87	0.01	0.07764	
Cell	53	13.1	13.1	0	0	
Cell	54	13.88	13.89	-0.01	-0.07205	

Cell	55	14.06	14.06	0	0	
Cell	56	13.43	13.43	0	0	
InterCB		16.1	16.07	0.03	0.186335	
InterCB		15.86	15.83	0.03	0.189155	
Begin	CB10					
Cell	57	13.16	13.15	0.01	0.075988	
Cell	58	13.83	13.83	0	0	
Cell	59	13.96	13.96	0	0	
Cell	60	14.25	14.24	0.01	0.070175	
Cell	61	14.2	14.19	0.01	0.070423	
Cell	62	16.13	16.14	-0.01	-0.062	
Begin	CB11					
Cell	63	17.08	17.09	-0.01	-0.05855	
Cell	64	13.79	13.8	-0.01	-0.07252	
Cell	65	15.03	13.76	1.27	8.449767	8.449767
Cell	66	12.97	12.97	0	0	
Cell	67	12.81	12.82	-0.01	-0.07806	
Cell	68	16.6	16.6	0	0	
Begin	CB12					
Cell	69	16.66	16.66	0	0	
Cell	70	13.48	13.48	0	0	
Cell	71	13.37	13.37	0	0	
Cell	72	14.67	13.17	1.5	10.22495	10.22495
Cell	73	16.47	16.43	0.04	0.242866	
Cell	74	14.42	14.42	0	0	